post-print for 2018 8th International Conference on Localization and GNSS (ICL - GNSS), 26-28 June 2018, Guimarães, Portugal

Opportunities and Challenges in the Industrial Internet of Things based on 5G Positioning

Yi Lu, Philipp Richter, Elena Simona Lohan
Tampere University of Technology, Finland
{yi.lu, philipp.richter, elena-simona.lohan}@tut.fi

***Abstract*—This paper discusses several features of 5G positioning in the context of applications for the Industrial Internet of Things (IIoT) which demand high accuracy of position information. The main opportunities to come with 5G networks, such as huge available spectrum, small cell networks, Multiple Input Multiple Output antennas and beamforming are summarized, and the challenges in the context of robot 5G positioning are pointed out. A case study for the localization of an indoor robot in a multi-wall multi-floor scenario is presented, based on various carrier frequencies and access node densities. We find out that sub-meter positioning accuracy required for most of the future industrial applications is theoretically achievable via a combination of small cell networks, mmWave carriers and antenna arrays, but practical issues such as node synchronization, connectivity and ultra dense network deployment costs have to be tackled.**

I. Introduction

With the fast advances of 5G standardization, several new opportunities are brought along, such as Augmented Reality (AR), eHealth, telepresence and Industrial Internet of Things (IIoT). Among those, in our opinion it is the IIoT that can benefit the most from the positioning capabilities of 5G networks, because position information can help to optimize and to automatize the processes in various vertical sectors, ranging from logistics and manufacturing to mining and transportation. It is usually understood that there are three main segments within the IIoT, namely the industrial control, the factory automation, and the process automation. Especially within the industrial control and factory automation segments, the positioning information is highly beneficial at both communication sides: for the (mobile) terminals (or robots) to accomplish their tasks and for the network to allocate and control the resources and to increase the processing efficiency.

IIoT applications are characterized by stringent requirements in terms of the quality, latency and reliability of the communication link as well as of the accuracy and precision of the positioning. These demands need to be met both indoors and outdoors, and typically over large coverage areas. Moreover, additional information about the surroundings, e.g. from sensor networks or maps, might be required such that, for example, the unmanned robots can navigate in a dynamic environment and autonomously accomplish their critical tasks within a manufacturing process. This paper outlines how different features of the 5G networks can improve the 5G positioning and it assesses their trade-off in the context of IIoT robot localization.

The goal of this paper is three-fold: first to present a survey of the opportunities and challenges in the IIoT localization based on 5G positioning; secondly, to present an analytical model for indoor path losses, shadowing, and Time of Arrivals (ToA) under Line of Sight (LoS) and Non Line of Sight (NLoS) conditions; and lastly, to show a case-study based on an indoor multi-floor multi-wall simulator for 3D positioning of a robot within cmWave and mmWave spectra. We will show the impact on the positioning accuracy of the indoor robot if we use mmWave signals, if we increase the AN (Access Node) density, and if we make use of MIMO antenna gains through beamforming.

II. 5G positioning

In this section, we discuss the benefits of various 5G network features in terms of achieving accurate and robust 5G positioning of the robots.

A. mmWave and beyond

The first benefits in 5G networks is the availability of a rich spectrum by utilizing the abundant mmWave band (i.e., spectrum larger than 30 GHz) which is not used in previous wireless communication system (i.e., 2G, 3G and 4G LTE). At mmWave, we have higher path loss and higher sensitivity to the atmosphere (absorption and penetration) [1] than at cmWave. The mmWave spectrum is therefore widely recognized to be used for short distance communications [2]. Certain transformations of the structure of networks have to be made to make use of mmWave at its full potential, and these will be discussed in the next subsections.

In terms of positioning benefits of the mmWave, higher accuracy and lower latency positioning of robots are made possible, due to more available signal bandwidth compared with cmWave spectrum. Specifically, a more accurate ToA (Time of Arrival) estimation in 5G positioning is enabled because of a finer delay domain resolution brought by the larger bandwidth, which at its turns leads to a more precise range estimation. Secondly, by leveraging the sparsity of the mmWave channel, the robot can in theory be localized with only one AN because multipath components can be converted to virtual anchors that contributes to the position estimate [3], [4].

However, a few challenges are incurred at the same time. Firstly, the positioning methods in 5G mmWave systems are quite opportunistic, especially with high mobility, i.e., the

communication quality as well as the positioning accuracy are closely tied to the environment, thus, the link reliability is highly context based. Also, several factors such as a poor geometry w.r.t. the ANs in view or temporary blockage of the LoS can have severe negative impact on the radio link.

Research beyond 5G also focuses on sub-mmWave band or TeraHertz (THz) bands, where the signal bandwidth will become even larger, antenna array size become even smaller (half-wavelength of 1 THz is only $150\,\mu$m which means, e.g., that a 128 elements antenna array only possesses a physical length of 19.2 mm). Therefore, massive MIMO will be enhanced to achieve further larger bandwidth and to reduce the interference. Moreover, the backhaul link of a network can take advantage of THz band in order to provide higher backhaul data rate than fronthaul [5]. Some of the challenges in THz bands (also sometimes referred to as "THz gap") are: extremely high path losses and atmosphere sensitivity, as well as large heat dispersion at antennas.

B. Small cell networks (SCNs)

The advantage brought in by the SCNs concept into the 5G positioning comes mainly from the fact that the SCNs can compensate the mmWave propagation loss. The severe path loss problem of mmWave can be addressed if the maximum distance between AN and robots (or terminals) within a single cell become shorter. Network densification is the key solution as it is much more easier for one AN to track a few (e.g., less than 10) robots than tens or hundreds of robots as in a conventional network (2G-4G). As such, the direct benefit to positioning brought by network densification is the potential to higher accuracy. The frequency reuse factor is also raised by using SCNs, yielding a high spectral efficiency. In addition, SCN can provide better cell-edge communication quality than conventional AN deployment, because the interference coming from adjacent cells is minimized due to high attenuation of mmWave signal.

In terms of positioning, SCNs enhance communication reliability and quality to any robot in indoor and urban areas, because when the mmWave signal from one AN is blocked, the robot can simply switch to a nearby ANs which has a better link quality. Thus, also the LoS probability increases in SCNs, which is considered as crucial in order to achieve sub-meter positioning accuracy. Moreover, SCNs can lead to a better positioning accuracy from the upper bound perspective: the radius of cell coverage defines a upper bound of absolute positioning error, therefore, small cells possess generally smaller radius that yields a smaller upper bound. In our simulator (Section IV), we model LoS probability according to the walls and the floors present in the propagation path and we investigate the average number of LoS connections per robot in a realistic multi-floor multi-wall scenario.

The main challenge coming with SCNs is the cost of backhaul communications and the backhaul routing algorithm among the ANs, further discussion of SCNs can be found in [6].

C. Massive MIMO

A third feature in 5G networks is the concept of massive MIMO, which lays the foundation of a high directional communication system by employing large antenna array techniques at both sides of the transmission chain. Massive MIMO provides a high energy efficiency thanks to a high directivity of the antenna arrays,a high spectrum efficiency due to large multiplexing gain, and a high reliability or robustness due to large diversity gain [7], [8]. The large multiplexing gain between the AN, on one hand, and the robot on the other hand, would enable the ultra high mobile broadband connection that 4G LTE cannot currently provide. Regarding to its benefits to positioning, massive MIMO offers a high directional beam which translates into a high SINR (Signal to interference noise ratio), which at its turn reduces the uncertainty of the ToA estimation. The highly directional link improves further the positioning and communications, by reducing the average number of multipath components received by the robot [8].

A challenge in massive MIMO is the signal processing algorithm complexity, due to the large number of antennas at both sides. Additionally, the acquisition of the channel state information (CSI) at AN on the downlink is rather difficult, as each robot has to estimate an amount of channel responses that is proportional to the number of AN antennas. This can be avoided if location-based beamforming (or geometric beamforming) is used [9].

D. Beamforming

Associated with massive MIMO, the beamforming (BF) technique, which is an array signal processing technique, makes the communications more efficient based on the awareness in the angular domain. Without antenna array and BF, the access nodes and the robots would acquire the signals in an omnidirectional ('blind') manner. This would make the multipaths to be a troublesome. As a result, the ToA measurements would be corrupted by multiple delays and the direction of arrival (DoA) estimation would not be possible. On the other hand, with BF, the high directional beam radiated by antenna array can be steered towards certain directions, forming dedicated transmission and reception at both sides. Not only can the high path loss and the interference coming from inter-cell and intra-cell be minimized, but also the ToAs from different paths become distinguishable. Thus, the DoA can be also estimated. As a consequence, with the ToA and DoA estimates, positioning can be carried out with a lower number of ANs compared to what is required by the RSS-based or ToA-based positioning system.

If also the robot is equipped with a BF capable multi-antenna system, the DoA and the Direction of Departure (DoD) can be estimated, facilitating the estimation of the robot's orientation with respect to the AN. By taking advantage of the sparsity of mmWave propagation channel, compressive sensing theory [4] can be used to efficiently estimate DoD and/or DoA which in turn contribute considerably to the positioning accuracy. Articles regarding BF based positioning application can be found in [9]–[12].

III. Positioning-related requirements and challenges in industrial applications

Table I summarizes the needed positioning-related features in various IIoT applications, according to the authors' view. Sub-m positioning accuracy is expected for the robot to be able to operate safely and reliably. A higher latency in positioning estimation is expected to be tolerated at smaller robot speeds.

The challenges related to positioning in industrial environments include:

- Device heterogeneity: many sensors and robot types available, some supporting only Received Signal Strength (RSS) measurements and some other supporting also ToA or DoA measurements.
- NLoS and multipath propagation: such situations introduce positioning errors in ToA and DoA estimates; solutions are, for example, to combine ToA/DoA information with other available information (e.g., visual reality, building maps, etc.).
- Synchronization issues: ToA-based positioning estimators typically rely on the assumption that the ANs are synchronized. Such synchronization is not always easy to achieve, especially with heterogeneous devices.
- Bandwidth and carrier frequency: the higher the available bandwidth, the more accurate positioning solutions can be found. For carrier frequencies above 30 GHz, currently more than 500 MHz contiguous bandwidths are available, while for carriers around 1–5 GHz, the available bandwidths are typically below 100 MHz. This points towards the advantage of employing mmWave signals for accurate positioning. On the other hand, the path losses are much higher at mmWave than at cmWave, which means that accurate positioning solutions are likely to be achieved only with a high AN density.

TABLE I
Positioning and navigation target requirements in industrial applications

Application	Indoor accuracy (cm)	Outdoor accuracy (cm)	Obstacle detection	Availability (%)	Latency (ms)
Indoor robot control	< 10	–	Yes	100	< 50
Outdoor robot control	–	< 30	Yes	100	< 10
Indoor item tracking	< 50	–	Yes	99	< 200
Outdoor item tracking	–	< 100	Yes	99	< 100
Remote control with AR	< 10	< 10	Yes	100	< 1

IV. Analytical modelling for indoor positioning

In this section, we introduce our indoor multi-floor multi-wall simulator that is based on a real building map with three floors. Two types of measurements are generated based on reasonable parameters and the geometry of the map, followed by a brief summary of the positioning method.

A. RSS-based positioning

The first positioning method is a RSS-based non-linear least square (NLS) estimator. The RSS $P_{a,i}$ from the a-th AN to the i-th robot is modelled according to a frequency-dependent multi-wall multi-floor model as follows,

$$P_{a,i} = \begin{cases} P_{T_a} - 20\log_{10}(f_{\text{c[Hz]}}) \\ \quad - 20\log_{10}(d_{a,i}) \\ \quad - 20\log_{10}\left(\frac{4\pi}{c}\right) + \eta_{\text{LOS}} & \text{if LOS} \\ P_{T_a} - 20\log_{10}(f_{\text{c[Hz]}}) \\ \quad - 20\log_{10}(d_{a,i}) \\ \quad - N_{iw_{a,i}} L_{iw} - N_{f_{a,i}} L_f \\ \quad - 20\log_{10}\left(\frac{4\pi}{c}\right) + \eta_{\text{NLOS}} & \text{if NLOS} \end{cases} \tag{1}$$

where P_{T_a} is the "apparent" transmit power of the a-th AN, (i.e., 'apparent' means here that we take into account all the cable losses and antenna gains at both ends), $f_{\text{c[Hz]}}$ is the considered carrier frequency, $L_{iw} = 10$ dB and $L_f = 20$ dB are the losses due to wall and floor attenuation (assumed constant within the building), $d_{a,i}$, $N_{iw_{a,i}}$ and $N_{f_{a,i}}$ are the distance, the number of walls and the number of floors between the a-th AN and the i-th robot, respectively. The speed of light is denoted by c, and η_{LOS} and η_{NLOS} express the shadowing for LoS and NLoS cases. The shadowing was modelled as a Gaussian-distributed variable with zero mean and standard deviation 2 dB for LoS cases and 6 dB for NLoS cases. The LoS cases were identified based on the building map, shown in Fig. 1: if there was no floor and no wall between the AN and robot, then we were in a LoS situation; if there was at least one floor or one wall on the AN–robot path, then we were in a NLoS situation. A receiver sensitivity of -110 dBm was assumed, meaning that signals received below this value are not heard, therefore, measurement from that specific AN will be discarded. We remark that our proposed model in eq. (1) is also similar to the indoor 3GPP channel models proposed for mmWave propagation [13].

B. ToA-based positioning

Here we assume perfectly synchronized ANs and robots and that the channel between ANs and robots is LoS-dominant (i.e., any multipath can be distinguished). Then, the ToA measurements from any arbitrary AN to any given robot (indices a, i have been dropped here for clarity) is modelled as

$$\tau_{\text{obs}} = \tau_{\text{true}} + b + v, \tag{2}$$

where $\tau_{\text{true}} = \|\mathbf{p}_{\text{r}} - \mathbf{p}_{\text{AN}}\|/c$, $\mathbf{p}_{\text{r}}$ and $\mathbf{p}_{\text{AN}}$ are the position vector of the robot and AN and v is a normally distributed random variable, $v \sim \mathcal{N}\left(0, \sigma^2_{\text{ToA}}\right)$. The term b reflects the NLoS bias (see fig. 2), which is related with the thickness of the obstacle, γ, as well as the relative permittivity, ε_r, [15]:

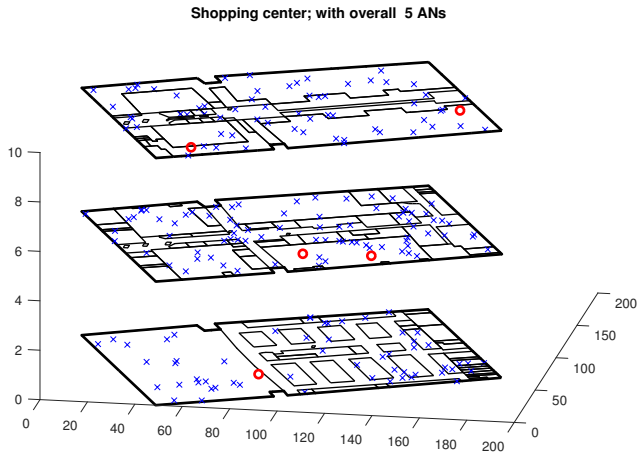

Fig. 1. The building map used in the simulator. Red circles show examples of AN location and blue crosses show examples of robot locations

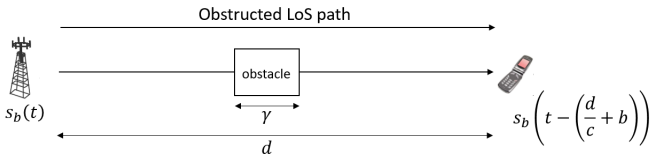

Fig. 2. LoS path blocked by an obstacle

$$b = \left(\sqrt{\varepsilon_r} - 1\right)\gamma/c \tag{3}$$

If the signal passes through N_{iw} walls and N_f floors to reach the robot, the whole bias is expressed as

$$b = \sum_{k=1}^{N_{iw}} \left(\sqrt{\varepsilon_{r,k}^{(w)}} - 1\right)\gamma_k/c + \sum_{j=1}^{N_f} \left(\sqrt{\varepsilon_{r,j}^{(f)}} - 1\right)\xi_j/c, \tag{4}$$

where $\varepsilon_{r,k}^{(w)}$ is the relative permittivity of the walls, γ refers to the thickness of the walls, $\varepsilon_{r,j}^{(f)}$ is the relative permittivity of the floors, and ξ refers to the thickness of the floors. The table of relative permittivity of typical construction materials can be found, for example, in [15], [16]. In our case study, the walls are assumed to be made of dry walls and the floors ceilings of solid concrete. It's worth pointing out that different choices of the materials lead to larger or smaller bias b, which affects the final positioning accuracy.

The last term in eq. (2) refers to the uncertainty of the ToA measurement which is caused by the noise v. To model the variance of the ToA, σ_{ToA}^2, we start with a typical multi-tap channel impulse response of a wireless channel, given as

$$h(t) = \sum_{i=0}^{L-1} \alpha_i \delta(t - \tau_i). \tag{5}$$

Let the transmit passband signal be $s(t) = \text{Re}\left\{s_b(t)e^{j2\pi f_c t}\right\}$, where $s_b(t)$ refers to the baseband signal, the received passband signal $y(t)$ can be expressed as

$$y(t) = \text{Re}\left\{\sum_{i=0}^{L-1} \alpha_i s_b(t - \tau_i) e^{j2\pi f_c (t-\tau_i)}\right\}. \tag{6}$$

The baseband receive signal $y_b(t)$ is therefore [17]:

$$y_b(t) = \text{Re}\left\{\sum_{i=0}^{L-1} \alpha_i s_b(t - \tau_i) e^{-j2\pi f_c \tau_i}\right\}. \tag{7}$$

All L taps are resolvable if we have a wide enough bandwidth available; and with known pilot signal and appropriate match filter, the attenuation factors $\alpha_i, i = 1, \ldots, L$ are omitted; therefore, ToA of each path is enveloped in the phase of the channel phasor $e^{-j2\pi f_c \tau_i}$ that is corrupted by AWGN only. The phase noise added on the channel phasor is modelled as a zero mean Gaussian random variable with variance [18]

$$\sigma_\theta^2 = \left[\frac{1}{2SNR}\left(1 + \frac{1}{2SNR}\right)\right] / (2\pi)^2. \tag{8}$$

Hence, the noise statistics of the ToA, σ_{ToA}^2, is obtained by dividing eq. (8) by f_c^2, yielding

$$\sigma_{\text{ToA}}^2 = \left[\frac{1}{2SNR}\left(1 + \frac{1}{2SNR}\right)\right] / (2\pi f_c)^2 \approx \frac{1}{8\pi^2 f_c^2 SNR}. \tag{9}$$

It's worth pointing out that the approximation in eq. (9) is equal to the CRB (Cramér-Rao Bound) of the variance of ToA estimate [19] if the product BT_s is close to 1. The signal bandwidth is denoted by B and T_s is the signal duration.

The SNR (in log-scale) in eq. (9) was computed as

$$SNR = P_{a,i} - N_0, \tag{10}$$

with $P_{a,i}$ given in eq. (1). The thermal noise power spectral density N_0 is given by $N_0 = -174 + 10\log_{10}(B) + NF$, and NF the receiver noise figure. We assumed that the available bandwidth B was equal at all carrier frequencies for a fair comparison, i.e., $B = 100$ MHz.

C. Positioning method

The positioning method applied here is based on NLS method [14]

$$\hat{\mathbf{p}} = \arg\min_{\mathbf{p}} \|\mathbf{m} - h(\mathbf{p})\|_2^2, \tag{11}$$

where $\mathbf{m}$ represents the measurements (RSS from eq. (1) or ToA from (2)) received by robots from a set of heard ANs and $\mathbf{p} = [x, y, z]$ is the robot position. The function $h(\cdot)$ refers to the deterministic part (including the corresponding bias) in eq. (1) for RSS measurements and eq. (2) for ToA measurements. Initial values for the NLS algorithm are computed with the centroid localization method [10], i.e. the initial position estimate of each robot is the centroid of all the heard ANs.

V. Simulation Results

Fig. 3 shows the average number of LoS connections in function of the total number of ANs in the building, distributed uniformly on each floor of the considered three-floor building. We used 1000 uniformly distributed random robot placements

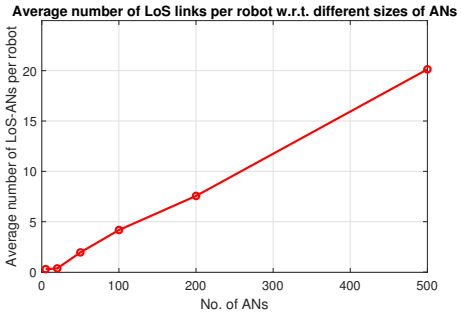

Fig. 3. Average number of LoS connections with different number of ANs

to compute this statistic. A LoS situation was counted when there were no walls and no floors between an AN and a robot. Clearly, if only 5 ANs are available in the whole building (three floors, with a floor surface equal to $183 \times 163 = 29.8 \cdot 10^3$ m^2), there are rather few LoS connections. However, if we have 50 or more ANs distributed uniformly in the building, we notice an average of around 2 LoS connections or more for each robot, which is the typical assumption of SCNs.

Fig. 4 shows the RMSE of the RSS-based and the ToA-based positioning methods at different carrier frequencies in cmWave and mmWave spectra and for three AN densities; namely i) when 5 ANs are available in the whole building (i.e., density about 55 ANs per km^2), ii) when 100 ANs are available in the whole building (i.e., density about 1113 ANs per km^2), and iii) when 500 ANs are available in the whole building (i.e., density about 5567 ANs per km^2). RSS-based estimates are rather independent of the carrier frequency and they do not achieve sub-meter accuracy, even with a very high density of ANs. On the other hand, the ToA-based estimators are becoming more accurate, both with an increased carrier frequency (explained by a lower variance in ToA estimates due to a higher root

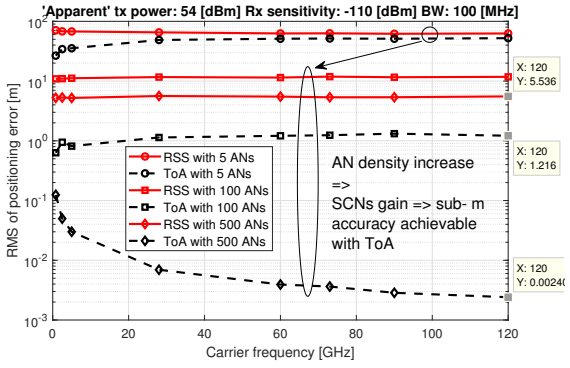

Fig. 4. RSS-based and ToA-based positioning accuracy under different AN densities

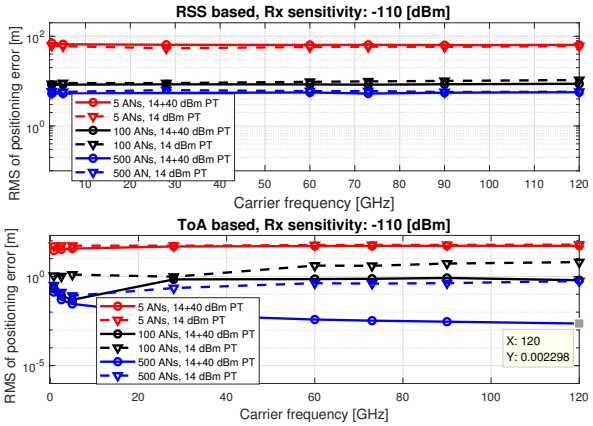

Fig. 5. RSS-based and ToA-based positioning accuracy under different AN densities and different array gains

mean square bandwidth at high carrier frequencies) and with an increased AN density. Nevertheless, in order to achieve a sub-meter accuracy needed for industrial applications, a very high AN density is required. In our case study about 500 ANs are required to yield sub-meter accuracy.

Fig. 5 shows the RMS of the positioning error versus the carrier frequency at two different apparent transmit powers, with RSS-based estimator and ToA-based estimator, respectively. In our study, there were 40 dB difference of apparent Tx power indicating an antenna array gain (i.e., MIMO gain). The obtained result reveals that even under a 40 dB MIMO gain, the accuracy of RSS-based estimates remains unchanged on average; whereas, the ToA-based estimator's accuracy improves, especially in dense network scenarios (i.e., higher than 100 ANs over 3 floors). A positioning accuracy of 2.3 mm, at 120 GHz, proves the benefits of 5G positioning, brought by the rich spectrum, MIMO, and SCNs. As seen in the bottom plot of Fig. 5, with the exception of the case with a very low number of ANs (i.e., 5), the ToA performance is highly improved with an increased antenna gain. We also remark that a similar positioning accuracy is achieved by either applying a high apparent Tx power (e.g., 54 dBm, i.e., high MIMO gain) and a moderate number of ANs (e.g., 100), or by applying a low apparent Tx power (e.g., 14 dBm) but increasing the number of ANs (e.g., 500). The tradeoff between the Tx power and AN density is an interesting future research direction, in order to estimate the overall costs of the network.

Finally, Fig. 6 presents the positioning performance of both RSS-based and ToA-based estimators as a function of the number of ANs deployed in the building. An apparent Tx power of 54 dBm was used (i.e., MIMO gain of 40 dB was included). Fig. 6 shows that, with increasing number of ANs, the error of the RSS-based estimator decreases only slightly, while the error of ToA-based estimator decreases significantly. An error threshold of 50 cm is plotted, in accordance with Table I. We see that in our case study we would need about 200 ANs to achieve 50 cm accuracy at mmWave and 100 ANs

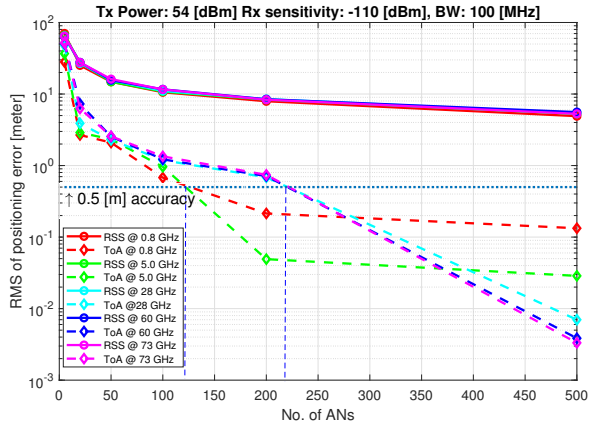

Fig. 6. RSS-based and ToA-based positioning accuracy as a function of the number of ANs

TABLE II
OPPORTUNITIES AND CHALLENGES OF 5G FOR WIRELESS POSITIONING IN INDUSTRIAL APPLICATIONS

5G feature	Opportunity	Challenge
mmWave	Accurate ToA estimation node synchronization	Link reliability
SCN	High LoS probability	Deployment cost
Massive MIMO	High SINR, i.e., less ToA uncertainty	Algorithm complexity
Beamforming	Accurate DoA/DoD estimation	Beam alignment cost

to achieve a similar accuracy at cmWave (assuming similar antenna gains, bandwidth and transmit powers). This is due to a higher path loss at higher carrier frequencies. Nevertheless, when SCNs and massive MIMO are exploited, positioning in mmWave spectrum promises higher accuracy than in cmWaves spectrum.

VI. CONCLUSION

In this paper we analyzed the opportunities and challenges for IIoT applications from different specific perspectives of 5G positioning and we presented a case study for 5G positioning of robots placed indoor in a multi-wall multi-floor building. A summary of this analysis is given in table II.

Our case study for indoor robot positioning showed that with SCNs (i.e., high AN density) and MIMO gain, a ToA-based estimator is able to achieve the sub-meter positioning accuracy needed for IIoT; additionally, an accuracy tradeoff between the apparent Tx power and the AN density was pointed out. Several technical challenges remain to be tackled, such as the AN–robot synchronization, attitude determination of robots, connectivity limitation, deployment costs of high density ANs. Future research will focus on ToA/DoA modelling and hybridization approaches for more accurate positioning with a moderate AN density.

ACKNOWLEDGEMENT

The authors express their warm thanks to the Academy of Finland (project 313039) for its financial support for this research work.

REFERENCES

[1] Z. Pi and F. Khan, An introduction to millimeter wave mile broadband system, in *IEEE Communications Magazine*, Vol. 49, no.6, pp. 101–107, June 2011.

[2] M. Marcus and B. Pattan, "Millimeter wave propagation; spectrum management implications," in *IEEE Microwave Magazine*, vol. 6, no. 2, pp. 54–62, June 2005.

[3] Klaus Witrisal, Stefan Hinteregger, Josef Kulmer, Erik Leitinger, Paul Meissner, "High-accuracy positioning for indoor applications: RFID UWB 5G and beyond", RFID (RFID) *2016 IEEE International Conference on*, pp. 1–7, 2016.

[4] J. Talvitie, M. Valkama, G. Destino, Henk Wymeersch, "Novel Algorithms for High-Accuracy Joint Position and Orientation Estimation in 5G mmWave Systems", in Proc. *IEEE Global Communications Conference, WI-UAV Workshop*, Dec. 2017.

[5] T. Narytnik, "The ways of creation and use of telecommunication systems in the terahertz band transport distribution 5G mobile networks", *2016 Third International Scientific-Practical Conf. Problems of Infocomm. Science and Technology (PIC ST)*, Kharkiv, pp. 36–39, 2016.

[6] M. Bennis, M. Simsek, A. Czylwik, W. Saad, S. Valentin and M. Debbah, "When cellular meets WiFi in wireless small cell networks," in *IEEE Comm. Magazine*, vol. 51, no. 6, pp. 44–50, Jun 2013.

[7] F. Rusek et al., "Scaling Up MIMO: Opportunities and Challenges with Very Large Arrays," in *IEEE Signal Processing Magazine*, vol. 30, no. 1, pp. 40–60, Jan. 2013.

[8] E. G. Larsson, O. Edfors, F. Tufvesson and T. L. Marzetta, "Massive MIMO for next generation wireless systems," in *IEEE Communications Magazine*, vol. 52, no. 2, pp. 186–195, February 2014.

[9] P. Kela et al., "Location Based Beamforming in 5G Ultra-Dense Networks," *2016 IEEE 84th Vehicular Technology Conference (VTC-Fall)*, Montreal, QC, 2016, pp. 1–7.

[10] M. Koivisto, A. Hakkarainen, M. Costa, P. Kela, K. Leppanen and M. Valkama, "High-Efficiency Device Positioning and Location-Aware Communications in Dense 5G Networks," in *IEEE Communications Magazine*, vol. 55, no. 8, pp. 188–195, 2017.

[11] G. Destino and H. Wymeersch, "On the trade-off between positioning and data rate for mmWave communication," *2017 IEEE International Conference on Communications Workshops (ICC Workshops)*, Paris, 2017, pp. 797–802.

[12] M. W. Khan, N. Salman and A. H. Kemp, "Cooperative positioning using angle of arrival and time of arrival," *2014 Sensor Signal Processing for Defence (SSPD)*, Edinburgh, 2014, pp. 1–5.

[13] 3rd Generation Partnership Project (3GPP), "Technical Specification Group Radio Access Network - Study on channel model for frequency spectrum above 6 GHz", 3GPP TR 38.900 V14.3.1 (Release 14), Jul 2017.

[14] Dennis, J. E. Jr. Nonlinear Least-Squares. State of the Art in Numerical Analysis, ed. D. Jacobs, Academic Press, pp. 269–312.

[15] C. Thajudeen, A. Hoorfar, F. Ahmad, and T. Dogaru, "Measured complex permittivity of walls with different hydration levels and the effect on power estimation of twri target returns," *Progress In Electromagnetics Research B*, Vol. 30, 177–199, 2011.

[16] J. Lu, D. Steinbach, P. Cabrol, P. Pietraski and R. V. Pragada, "Propagation characterization of an office building in the 60 GHz band," *The 8th European Conference on Antennas and Propagation (EuCAP 2014)*, The Hague, 2014, pp. 809–813.

[17] D. Tse, P. Viswanath, Fundamentals of Wireless Communications., Cambridge Univ. Press, 2005.

[18] Y. Lu, G. Seco-Granados, J.A. Lopez-Salcedo, "Kalman filter-based tracking for GNSS space receivers at high orbits", *Proc. 6th International Colloquium on Scientific and fundamental aspects of GNSS/Galileo*, Oct 2017.

[19] N. Patwari, J. N. Ash, S. Kyperountas, A. O. Hero, R. L. Moses and N. S. Correal, "Locating the nodes: cooperative localization in wireless sensor networks," in *IEEE Signal Processing Magazine*, vol. 22, no. 4, pp. 54–69, July 2005.